Top Catal (2009) 52:1709–1712
DOI 10.1007/s11244-009-9330-1

ORIGINAL PAPER

Effect of the Proximity of Pt to Ce or Ba in Pt/Ba/CeO_2 Catalysts on NO_x Storage–Reduction Performance

Robert Büchel · Reto Strobel · Alfons Baiker · Sotiris E. Pratsinis

Published online: 10 July 2009

Abstract The effect of Pt location in Pt/Ba/CeO_2 catalysts for NO_x storage–reduction (NSR) was analyzed. The Pt location on $BaCO_3$ or CeO_2 support was controlled by changing the angle (φ) between the two flame sprays producing these two components. As-prepared flame-made catalysts contain PtO_x which must be reduced during the fuel rich phase to become active for NO_x storage and reduction of NO_x. For Pt on $BaCO_3$ this process was significantly faster than for Pt on CeO_2. The increased reduction ability of Pt on Ba is reflected in the light off temperatures: for Pt on CeO_2 temperatures around 330 °C were needed to combust 20% of C_3H_6 in air while for Pt on $BaCO_3$ only 250 °C were required for the same conversion. The ability to control the location of Pt or other noble metals is, therefore, essential to optimize the catalysts for a given Pt/Ba/CeO_2 weight ratio. The best performance was observed when most of the Pt constituent was located near Ba-containing sites.

R. Büchel · R. Strobel · S. E. Pratsinis (✉)
Particle Technology Laboratory, Department of Mechanical and Process Engineering, ETH Zurich, Sonneggstrasse 3, Zurich 8092, Switzerland
e-mail: sotiris.pratsinis@ptl.mavt.ethz.ch

R. Büchel · A. Baiker
Department of Chemistry and Applied Biosciences, Institute for Chemical and Bioengineering, ETH Zurich, Wolfgang-Pauli-Strasse 10, Zurich 8093, Switzerland

Present Address:
R. Strobel
Satisloh Photonics AG, Horgen 8812, Switzerland

Keywords NO_x storage–reduction · Flame synthesis · Lean NO_x trap · Barium carbonate · Ceria · Platinum location

1 Introduction

Catalysts for NO_x storage–reduction (NSR) are attractive for exhaust gas treatment from fuel lean engines [1]. Under such conditions, exhaust NO_x is oxidized over a noble metal (Pt) and then trapped (stored) on an alkaline-earth or alkali metal (e.g., Ba or K) in the form of metal-nitrates [2]. During the subsequent short fuel rich period, NO_x originating from decomposition of the metal-nitrates are reduced on the noble metal to N_2 and the storage–reduction cycle restarts [3]. The major drawback of NSR catalysts is the high sensitivity to sulfur poisoning as sulfates of the storage material are formed (i.e., $BaSO_4$) which are more stable than the corresponding nitrates, requiring high regeneration temperatures (>800 °C) to decompose them [4]. At these temperatures, thermal deterioration occurs by particle growth, loss of surface area, and formation of mixed oxides (i.e., $BaAl_2O_4$) with a low NO_x storage capacity [5].

This problem can be circumvented by using support materials that either do not form mixed oxides with the storage material or only form mixed oxides that easily decompose in the presence of CO_2 or NO_x [5]. The proximity between Pt and Ba in Pt/Ba/Al_2O_3 affects the storage–reduction behavior through the spillover of NO_x [6]. With a two-nozzle flame spray pyrolysis (FSP) system active NSR material can be produced [7] controlling the Pt deposition on the support or storage material [8]. Here, we have elucidated the effect of Pt location in Pt/Ba/CeO_2 catalysts on their NSR behavior by controlling the angle φ between the two-nozzles in the FSP process. Ceria is

well-known for its ability to store and release oxygen [9] but is also promoting PtO_x formation [10].

2 Experimental

2.1 Apparatus and Preparation

Catalysts of $Pt/Ba/CeO_2$ were prepared using a two-nozzle FSP set up (Fig. 1) [7]. The inter nozzle distance (d) was constant 6 cm while the angle φ was changed from 100 to 160° corresponding to a mixing distance (m) of 7 cm to 34 cm, with $m = d \cdot \tan(\varphi/2)$. The individual spray nozzles were described previously in detail [11]. The Ce-precursor solution consisted of Ce 2-ethylhexanoate (Alfa Aesar, 49% in 2-ethylhexanoic acid) dissolved in a 1:1 vol% mixture of toluene (Riedel-de Haën, 99%) and 2-ethyl hexanoic acid (Riedel-de Haën, 95%). The Ce concentration was kept constant at 0.2 mol/L. The appropriate amount of Ba 2-ethylhexanoate (Aldrich, 98%) was dissolved in 1:1 vol% toluene (Riedel-de Haën, 99%) and 2-ethylhexanoic acid (Riedel-de Haën, 95%). The Pt-precursor, platinum(II) acetylacetonate (STREM, 98%), was added either to the Ba- or Ce-precursor solutions. The concentration of the metals in the two liquid solutions was chosen to result in a nominal $Pt:Ba:CeO_2$ weight ratio of 1:20:100 in the powder.

The Ba-precursor was fed at 3 mL/min through the first nozzle and the Ce-precursor was fed at 5 mL/min through the second nozzle. Each solution was dispersed with 5 L/min oxygen (PanGas, 99.95%) forming a fine spray being ignited by a supporting premixed methane/oxygen flame with a CH_4/O_2 ratio of 0.5 and a total gas flow of 3 L/min. The produced powder was collected on a glass fiber filter (Whatman GF6, 25.7 cm in diameter) with the aid of a vacuum pump (Busch, Seco SV 1040C).

The designation used here indicates the component on which Pt is deposited: catalyst with Pt on Ba is referred to as Ce–BaPt, and Pt on CeO_2 as PtCe–Ba.

2.2 Materials Characterization

The specific surface area (SSA) of the as-prepared powders was determined by a five-point nitrogen adsorption isotherm at 77 K using the BET method [12]. X-ray diffraction (XRD) patterns were recorded with a Bruker D8 Advance instrument (40 kV, 40 mA, $\lambda = 1.54$ nm) at a scan speed of 0.5°/min at $10° < 2\theta < 70°$ and analyzed based on the fundamental parameter approach and the Rietveld [13] method with the TOPAS 3 software using $BaCO_3$ (ICSD 63257) and CeO_2 (ICSD 72155). The Pt dispersion was measured by CO-pulse chemisorption at 40 °C on a Micromeritics Autochem II 2920 [14]. The NSR measurements were performed with 20 mg of catalyst in a fixed-bed reactor (with an inner diameter of 4 mm) for a constant NO inlet. The reactor was connected to a valve device allowing rapid switching between oxidizing (6.6% O_2 and 666 ppm NO in He) and reducing conditions (1333 ppm C_3H_6 and 666 ppm NO in He) [10]. The NO_x and NO concentrations in the effluent gas were monitored using a chemiluminescence detector (ECO Physics, CLD 822S). The NO_x conversion for a full cycle (one storage and one reduction) was derived from the corresponding NO_x outlet concentration according to the following equation:

$$NO_x \text{ conversion} = \frac{NO_{x,in} - NO_{x,out}}{NO_{x,in}} \times 100\% \quad (1)$$

3 Results and Discussion

3.1 Powder Characterization

Figure 1 shows the 2-FSP setup used for synthesis of $Pt/Ba/CeO_2$. The angle φ between the two-nozzles was changed and Pt was added either to the Ce or to the Ba-precursor. X-ray diffraction (XRD) analysis (not shown) indicated that neither the angle φ nor the Pt position had an influence on the crystal structure of the powders [8]. The crystals detected were face centered cubic CeO_2, with an average crystal size of 9 nm, and monoclinic $BaCO_3$, with a crystal size of 12 nm. No Pt was detected, as its concentration and particle size were below the detection limit of the XRD. The metastable monoclinic $BaCO_3$ transforms within a week into the more stable orthorhombic $BaCO_3$ as reported previously [15]. The specific surface area was decreasing for smaller angles φ (Fig. 2), the smallest specific surface area was 117 m^2/g for $\varphi = 100°$ and the highest for $\varphi = 160°$ was 130 m^2/g. With decreasing φ the distance m is decreased exposing the particles to higher temperatures favoring their growth by coagulation and sintering. The addition of Pt had no influence on the specific surface area as

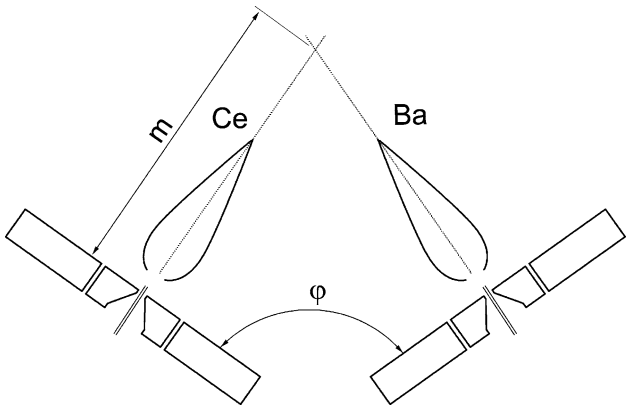

Fig. 1 Schematic of the two-nozzle FSP unit. Pt is either added to the $BaCO_3$ or the CeO_2 producing nozzle

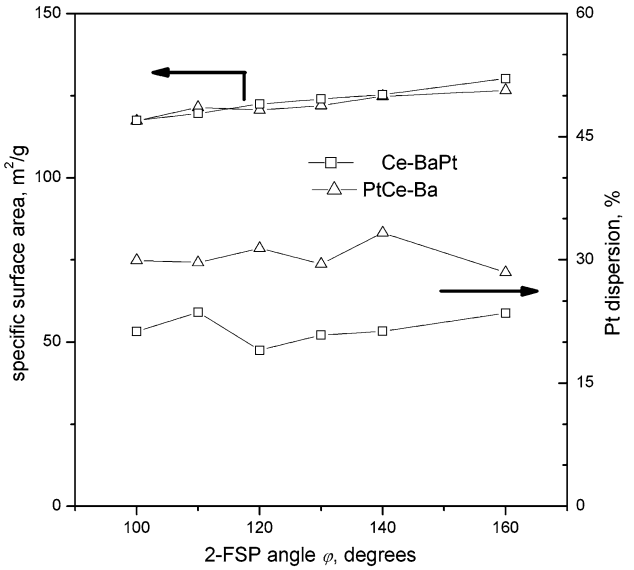

Fig. 2 The specific surface area (SSA) of produced catalysts and the corresponding Pt dispersion as a function of 2-FSP angle φ

shown in Fig. 2 where the PtCe–Ba and the Ce–BaPt curves overlap. The Pt dispersion, however, was higher for Pt on Ce (30%) compared to Ce–BaPt (25%). This was attributed to the lower SSA of the $BaCO_3$ species [8] as a similar tendency was observed for $Pt/Ba/Al_2O_3$ [8].

3.2 Catalytic Performance

For a constant NO inlet Fig. 3a shows the NO_x outlet concentration for PtCe–Ba and Ce–BaPt at $\varphi = 160°$, while changing between fuel lean and fuel rich atmospheres (cycles) at a reactor temperature of 350 °C. For Ce–BaPt the NO_x outlet concentration starts at zero after each fuel lean/rich cycle and about the same amount of NO_x was stored during the fuel lean cycles as Pt is known to promote $Ba(NO_3)_2$ regeneration by decreasing its thermal stability [16]. PtCe–Ba in contrast showed higher outlet NO_x concentrations and after the fuel rich cycle the outlet NO_x did not return to zero, an indication that the stored nitrates were not, or only insufficiently regenerated. Good regeneration, however, is essential for NSR catalysts which run for a longer time period in order to maintain high fuel efficiency. When changing from fuel lean to fuel rich conditions, higher NO_x outlet than NO inlet concentrations were detected. This effect, called overshooting, had been observed before [10] and was attributed to CO_2 promoted NO_x release [17]. In Ce–BaPt higher NO_x overshooting than in PtCe–Ba was observed indicating a higher Pt activity. Such high peak concentration, however, are undesired in technical catalysts, as they are lowering the NO_x conversion efficiency and furthermore peak concentrations are typically restricted by federal laws.

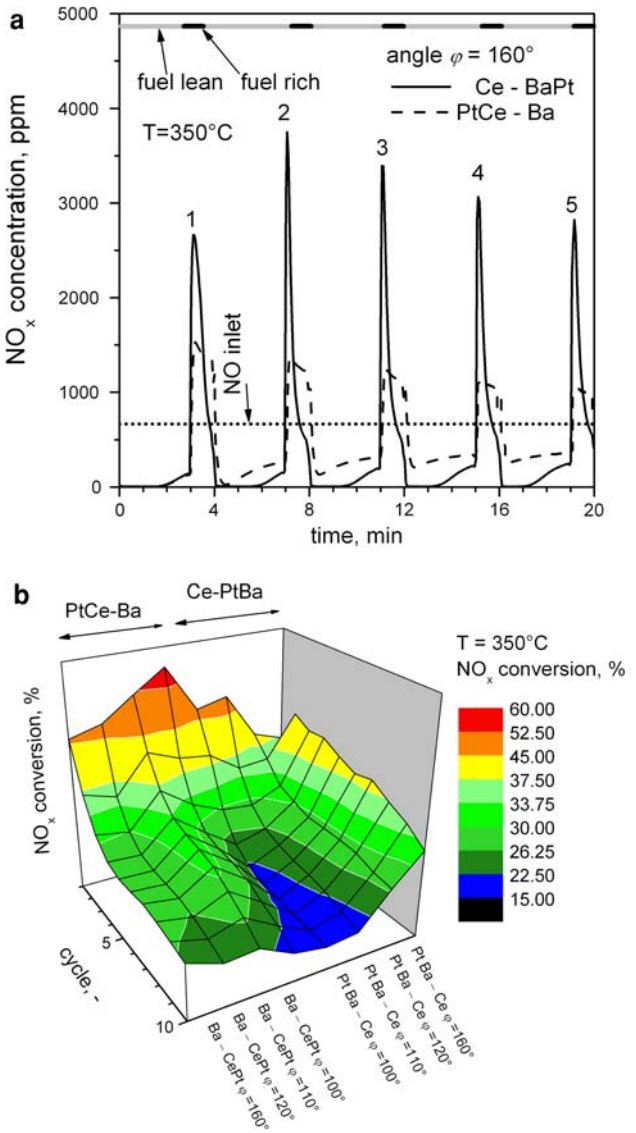

Fig. 3 **a** NO outlet concentration for $\varphi = 160°$ for Pt on CeO_2 (PtCe–Ba) and Pt on Ba (Ce–BaPt) at $T = 350$ °C. **b** NO_x conversion with Pt on CeO_2 or $BaCO_3$ support at 350 °C at various 2-FSP angles and number of NSR cycles

In Fig. 3b the NO_x conversion according to Eq. 1 is summarized for different φ as a function of the number of cycles at 350 °C. On the Ce–BaPt side, the NO_x conversion decreases for small φ. This behavior is attributed to the decrease of SSA (see Fig. 2) and the fact that more Pt deposited also on CeO_2 forming undesired PtO_x species. At small angles (e.g., $\varphi = 100°$) the effect of the addition of Pt to Ce- or Ba-precursor was less significant, because Pt formation was taking place after Ba/Ce were mixed and consequently Pt deposited on both components indiscriminately. As for the PtCe–Ba, the NO_x conversion was not much affected by the angle and therefore was more or less constant as PtCe–Ba did not regenerate the stored NO_x and only stored NO until the storage capacity of Ba had been

reached. The reason for this behavior could be that the Pt on CeO_2 was oxidized and an insufficient amount of C_3H_6 was combusted at 350 °C. For both powders made at $\varphi = 160°$, the PtCe–Ba shows a higher NO_x conversion in the first cycle. In the following cycles, however, the performance of PtCe–Ba is decreasing significantly, compared to Ce–BaPt, as insufficient regeneration of the $Ba(NO_3)_2$ takes place when Pt is separated from the Ba compound [16].

3.3 Combustion of C_3H_6

The reduction ability of the catalysts was investigated by measuring the light off temperature (T_{20}) needed to combust 20% of C_3H_6 in an oxygen rich atmosphere as shown in Fig. 4. Ce–BaPt was more active as its T_{20} is 100 °C lower than that of PtCe–Ba. With decreasing φ, the T_{20} of the Ce–BaPt increased and consequently less C_3H_6 was combusted at 350 °C. Thus, it can be assumed that at this temperature also the activity of Pt for reducing NO_x to N_2 was insufficient, as seen in Fig. 3a and b. PtCe–Ba showed an almost constant T_{20} of 330 °C, possibly because of PtO_x formation promoted by the CeO_2 [9, 10]. The higher oxidation level of Pt in PtCe–Ba was further indicated by the powder color. While PtCe–Ba had a reddish color, catalysts with Pt on the Ba side (Ce–BaPt) were lightly yellow. Because the support CeO_2 and $BaCO_3$ are white, this color change must be associated with the Pt itself. In the reduced form, for example after H_2 treatment, the catalysts could not be distinguished by the color as they both were silver-black.

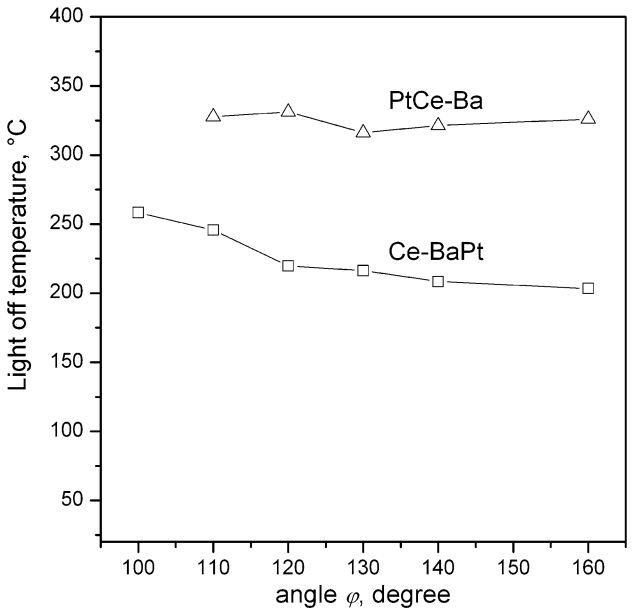

Fig. 4 Light off temperature to combust 20 mol.% C_3H_6 as a function of 2-FSP angle φ

4 Conclusions

$Pt/Ba/CeO_2$ catalysts were produced with a 2-FSP setup. Preferential deposition of Pt on Ba or CeO_2 was achieved by controlling the angle φ between the FSP nozzles, changing the meeting distance of the two flame plumes. The specific surface area of the particles decreased up to 10% by decreasing φ as the two plums mixed earlier affording higher flame temperatures that increased the catalyst particle size. Pt oxides were formed when Pt was deposited on CeO_2 because this support is a good oxidation and oxygen storage agent limiting the reduction of NO_x. For good NO_x conversion, however, a fast regeneration during the fuel rich part of the NSR was essential. Pt in close proximity to Ba formed much less Pt oxides and therefore, showed better NSR performance and a low light off temperature for C_3H_6 combustion.

Acknowledgments We kindly acknowledge financial support by ETH Zürich (TH-09 06-2) and thank the contribution of platinum chemicals by Johnson Matthey PLC.

References

1. Miyoshi N, Matsumoto S, Katoh K, Tanaka T, Harada J, Takahashi N, Yokota K, Sugiura M, Kasahara K (1995) SAE Technical Paper 950809
2. Takahashi N, Shinjoh H, Iijima T, Suzuki T, Yamazaki K, Yokota K, Suzuki H, Miyoshi N, Matsumoto S, Tanizawa T, Tanaka T, Tateishi S, Kasahara K (1996) Catal Today 27:63
3. Fritz A, Pitchon V (1997) Appl Catal B 13:1
4. Epling WS, Campbell LE, Yezerets A, Currier NW, Parks JE (2004) Catal Rev Sci Eng 46:163
5. Casapu M, Grunwaldt JD, Maciejewski M, Wittrock M, Gobel U, Baiker A (2006) Appl Catal B 63:232
6. Cant NW, Liu IOY, Patterson MJ (2006) J Catal 243:309
7. Strobel R, Madler L, Piacentini M, Maciejewski M, Baiker A, Pratsinis SE (2006) Chem Mater 18:2532
8. Büchel R, Strobel R, Krumeich F, Baiker A, Pratsinis SE (2009) J Catal 261:201
9. Kaspar J, Fornasiero P, Graziani M (1999) Catal Today 50:285
10. Strobel R, Krumeich F, Pratsinis SE, Baiker A (2006) J Catal 243:229
11. Madler L, Stark WJ, Pratsinis SE (2002) J Mater Res 17:1356
12. Brunauer S, Emmett PH, Teller E (1938) J Am Chem Soc 60:309
13. Cheary RW, Coelho AA (1998) J Appl Crystallogr 31:851
14. Piacentini M, Strobel R, Maciejewski M, Pratsinis SE, Baiker A (2006) J Catal 243:43
15. Strobel R, Maciejewski M, Pratsinis SE, Baiker A (2006) Thermochim Acta 445:23
16. James D, Fourre E, Ishii M, Bowker M (2003) Appl Catal B Environ 45:147
17. Amberntsson A, Persson H, Engstrom P, Kasemo B (2001) Appl Catal B 31:27